Supporting information

# Hourglass-type Polyoxometalate-based Crystalline Materials as Efficient Cooperating Photocatalysts for the Reduction of Cr(VI) and Oxidation of Dye

Xuerui Tian, Yaqi Zhang, Yuanyuan Ma*, Qing Zhao and Zhangang Han*

Hebei Key Laboratory of Organic Functional Molecules; National Demonstration Center for Experimental Chemistry Education; College of Chemistry and Material Science, Hebei Normal University, Shijiazhuang, Hebei 050024, People's Republic of China

* Corresponding author. E-mail: mayy334@hebtu.edu.cn, hanzg116@126.com

**List:**

## 1. Experimental Section

**Standard curves of photocatalytic reduction of Cr(VI) and oxidation of MB**

When the incident light, absorption coefficient and path length keep same, the transmitted light only changes with the concentration of the solution. So, in a certain range, the concentration $c$ and absorbance $A$ accord with the Lambert's law:

$$A = \kappa bc. \quad (1)$$

So its conversion rate can also be expressed as follows:

$$D = (A_0 - A_t) / A_0 \times 100\%. \quad (2)$$

Where D is the conversion, $A_0$ is the initial solution absorbance, and $A_t$ is the solution absorbance at reaction time t (min).

Excess FA, if the reduction of Cr (VI) follows pseudo first-order kinetics, the rate constant k and reaction time t can be determined using the following equation:

$$\lg c_t\,(A) = \lg c_0\,(A) - kt / 2.303 \quad (3)$$

The Arrhenius equation $k = Be^{-Ea/RT}$ is then changed into:

$$\lg k = -Ea/2.303RT + \lg B;$$

where

$$E_a = -19.15 \times k(\text{slope})$$

B is the pre-exponential factor, $E_a$ is the apparent activation energy, and $R$ and $T$ are the gas constant and thermodynamic temperature (K), respectively.

## 2. Supplementary Figures

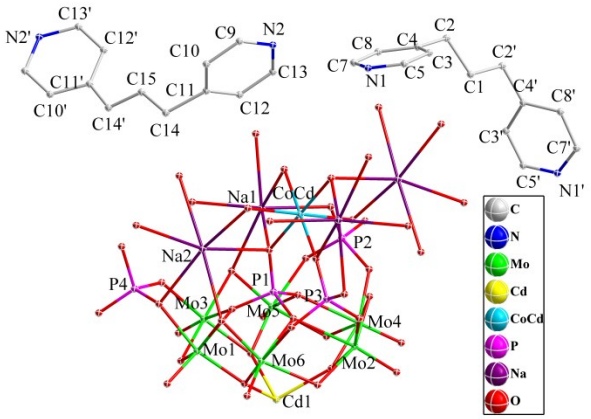


**Fig. S1** Simplified diagram of the asymmetric unit of compound **1**.

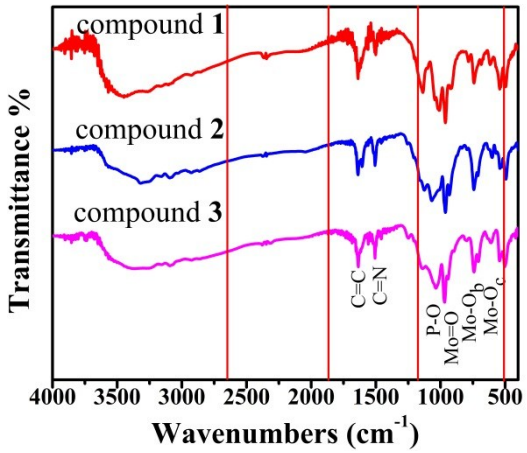


**Fig. S2** IR spectra of **1-3** showing the different characteristic bands for polyanions and organic components.

IR spectra of compounds **1-3** were measured and exhibited the similar characteristic peaks at 4000-400 $cm^{-1}$ (Fig. S2). The peaks at 1015~1070 $cm^{-1}$ are attributed to anti-symmetric vibrations of $\nu_{as}(P\text{-}O_a)$. The $\nu(Mo{=}O_t)$ stretching vibration are in the vicinity of 960 $cm^{-1}$, and the strong peaks at 600~750 $cm^{-1}$ are ascribed to the characteristic absorption peak of ν(Mo-O) stretching vibration. The absorption peaks located near 1500~1600 $cm^{-1}$ are the stretching vibration of C=C and C=N bonds from the organic part of the three compounds. Furthermore, the broad peaks at 3250~3440 $cm^{-1}$ are assigned to the stretching vibration of ν(O-H), ν(C-H) and ν(N-H).

| | Elements | Weight % | Atom % |
|---|---|---|---|
| Compound **1** | C K | 17.08 | 26.00 |
| | O K | 59.20 | 67.65 |
| | P K | 3.12 | 1.84 |
| | Mo L | 18.10 | 3.45 |
| | Na K | 0.89 | 0.71 |
| | Cd L | 1.04 | 0.17 |
| | Co K | 0.56 | 0.18 |
| | Sum | 100.00 | - |
| Compound **2** | C K | 36.62 | 48.64 |
| | O K | 47.98 | 47.84 |
| | P K | 2.76 | 1.42 |
| | Mo L | 11.77 | 1.96 |
| | Cd L | 0.72 | 0.10 |
| | Zn K | 0.15 | 0.04 |
| | Sum | 100.00 | - |
| Compound **3** | C K | 23.83 | 38.99 |
| | O K | 41.63 | 51.14 |
| | P K | 5.79 | 3.67 |
| | Mo L | 25.60 | 5.24 |
| | Cd L | 2.44 | 0.43 |
| | Al K | 0.72 | 0.52 |
| | Sum | 100.00 | - |

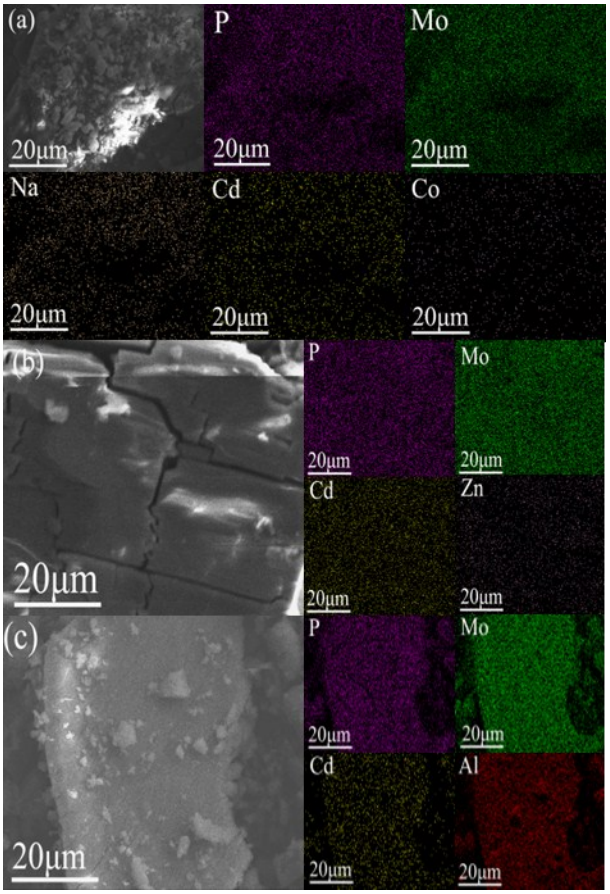


**Fig. S3** EDS analysis results for representative elements in the relevant regions of compounds **1**(a), **2**(b) and **3**(c).

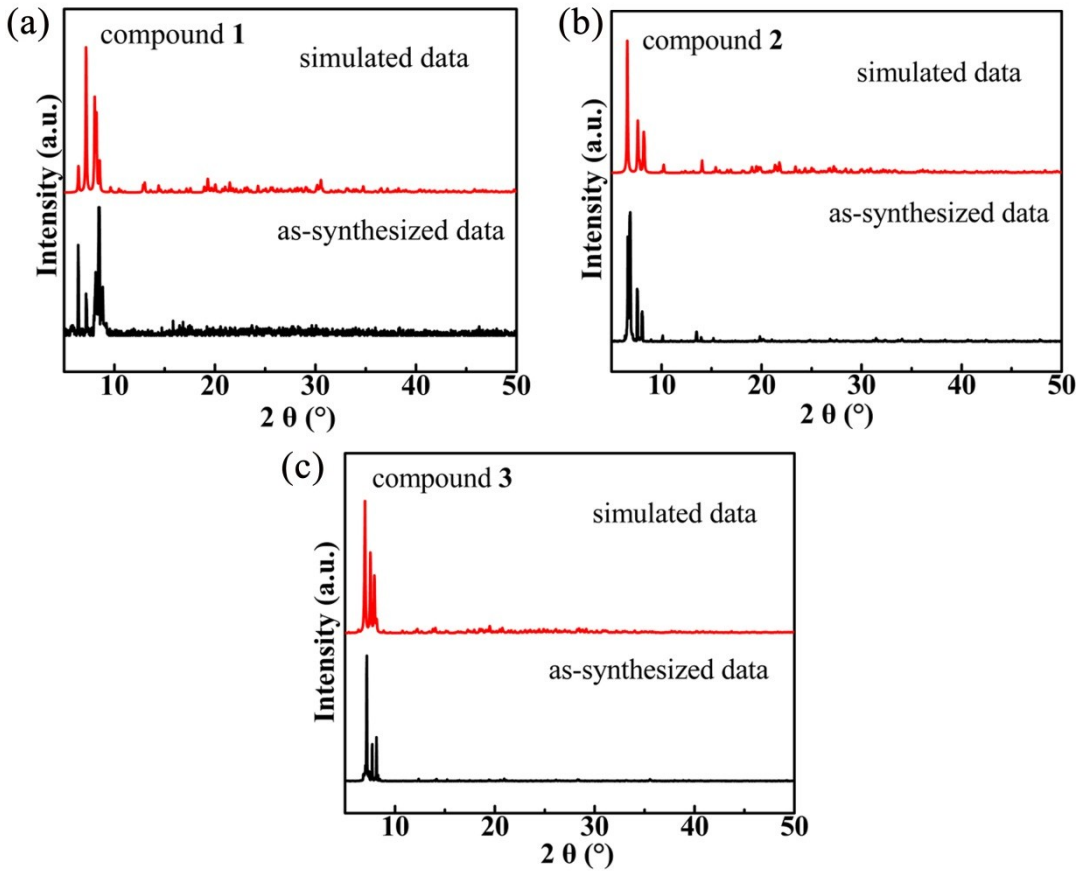


**Fig. S4** The XRD patterns of compounds **1-3**.

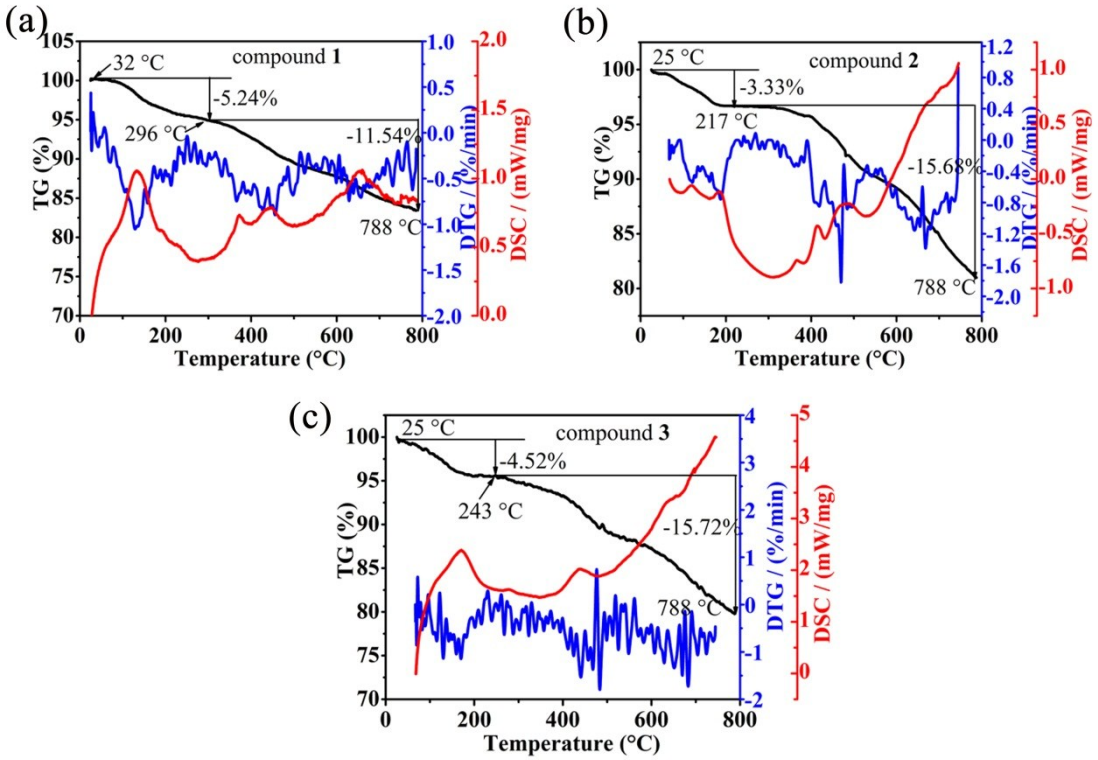


**Fig. S5** TG, DTG and DSC curves for compounds **1-3**.

Thermogravimetric analysis of compounds **1-3** were carried out under a $N_2$ atmosphere from 20 to 800 °C. As seen from Fig. S5, TG curves of **1-3** exhibited the two weight-loss steps between 25 °C and 788 °C. Compound **1** has the actual weight loss of 5.24% (theoretical value 5.00%) in the range of 32-296 °C, which is equivalent to the loss of 2 crystal water and 7 coordination water molecules from metal Na/Cd/Co; the second step weight loss range at 296-788 °C, the actual weight loss is 15.54% (theoretical value 12.37%), which is equivalent to the loss of all protonated organic components. The TG-DSC curves of compound **2** showed that the weight loss from 25 °C to 217 °C is *ca.* 3.33% and is equivalent to the loss of lattice water (theoretical value: 3.22%), as the temperature rises to 788 °C, almost all of the protonated organic components are lost. At the same time, it can be seen from the figure that the inorganic frame structure remains intact even at very high temperatures. Similarly, for compound **3**, the overall weight loss is *ca.* 20.24% from 25 up to 788 °C, attributed to the loss of crystal waters and organic components (theoretical value: 19.54%).

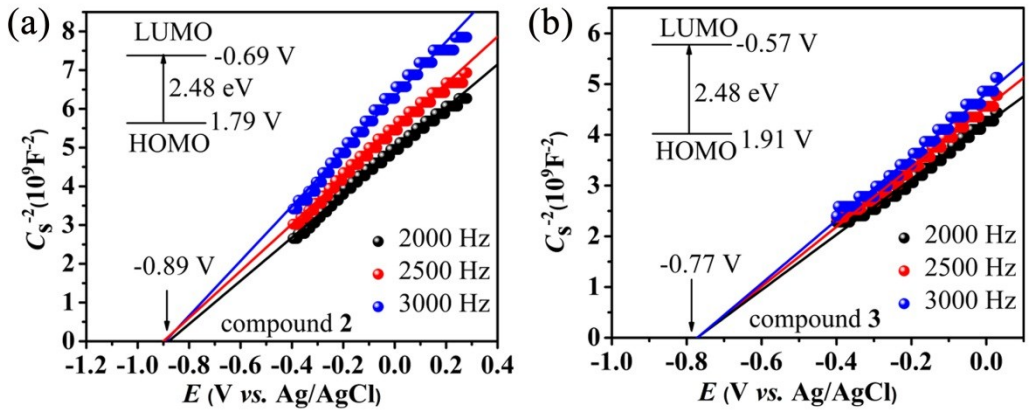


**Fig. S6** Mott-Schottky plot of compounds **2-3** in 0.2 M $Na_2SO_4$ solution at pH = 6.80. Inset: Energy diagram of the HOMO and LUMO levels of **2-3**.

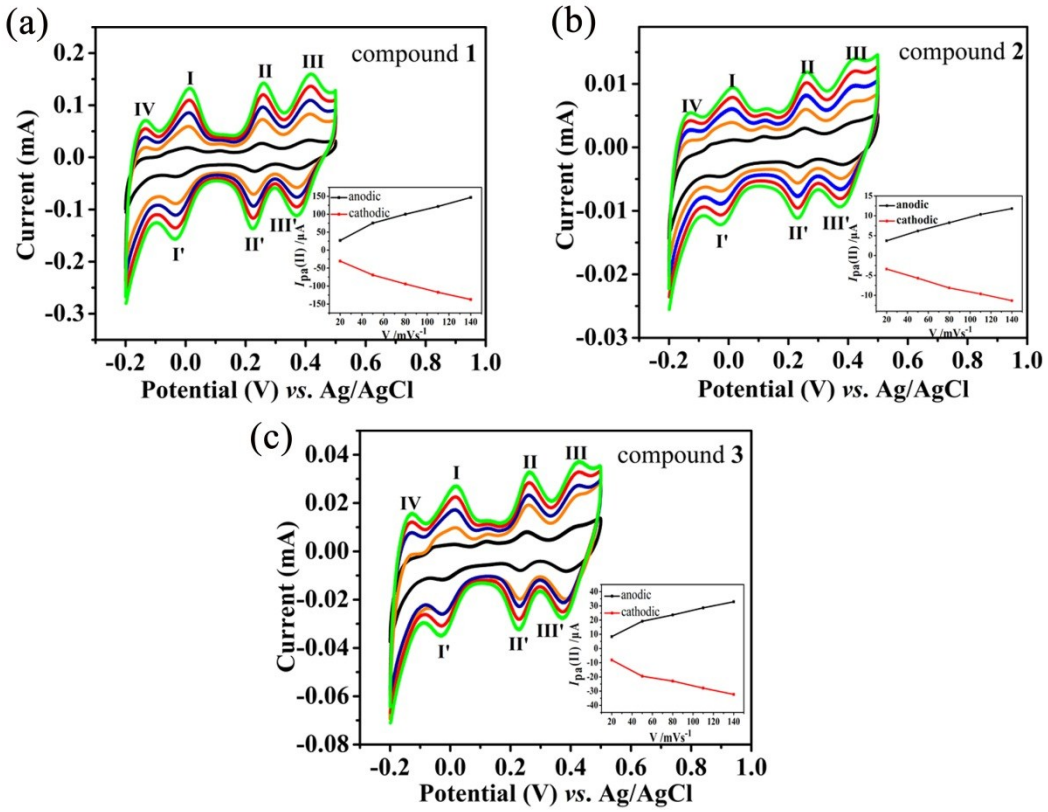


**Fig. S7** Cyclic voltammograms of **1-3** with different sweep rates (20, 50, 80, 110, 140 mV·s$^{-1}$) in 1M $H_2SO_4$ solution. Inset is plot of peak current vs. scan rate for peak (I-I').

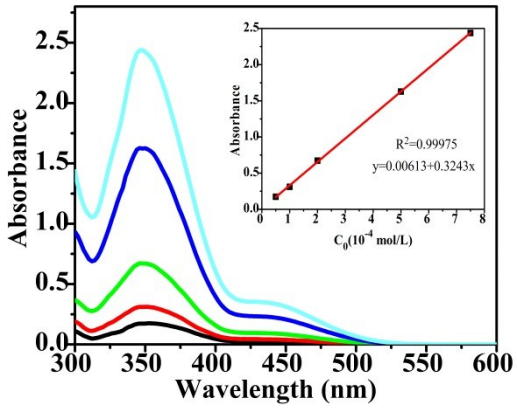


**Fig. S8** UV absorption spectra of different concentrations of Cr(VI) solution (mass concentration from the inside out were $0.1 \times 10^{-4}$, $1 \times 10^{-4}$, $5 \times 10^{-4}$, $8 \times 10^{-4}$, $10 \times 10^{-4}$ mol / L). The internal graph shows the relationship between the mass concentration of Cr(VI) solution and absorbance at a wavelength of 348 nm.

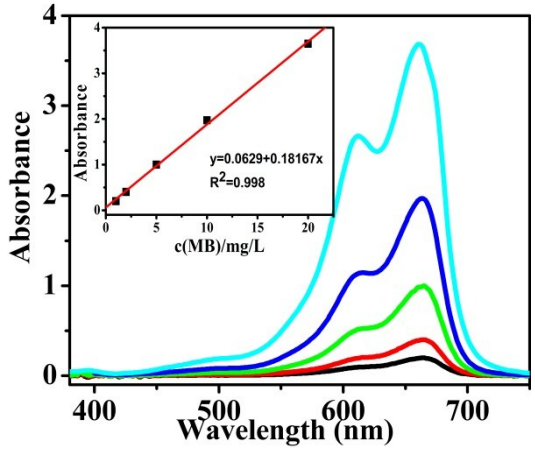


**Fig. S9** UV absorption spectra of MB solutions with different mass concentrations (mass concentration is 1, 2, 5, 10, 20 mg/L from the inside out); internal plot is the mass concentration and absorbance of MB solution at 662 nm.

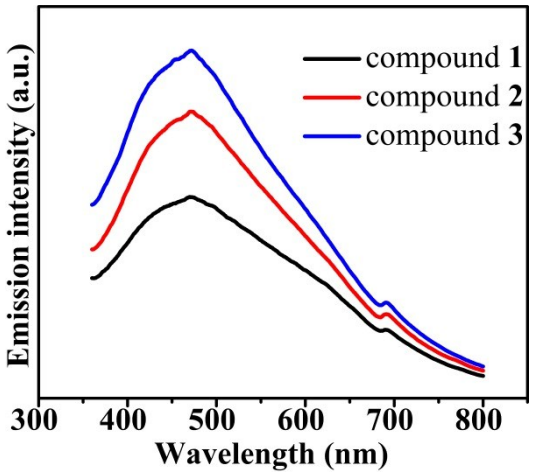


**Fig. S10** Emission spectra of compounds **1-3** (solid) at room temperature.

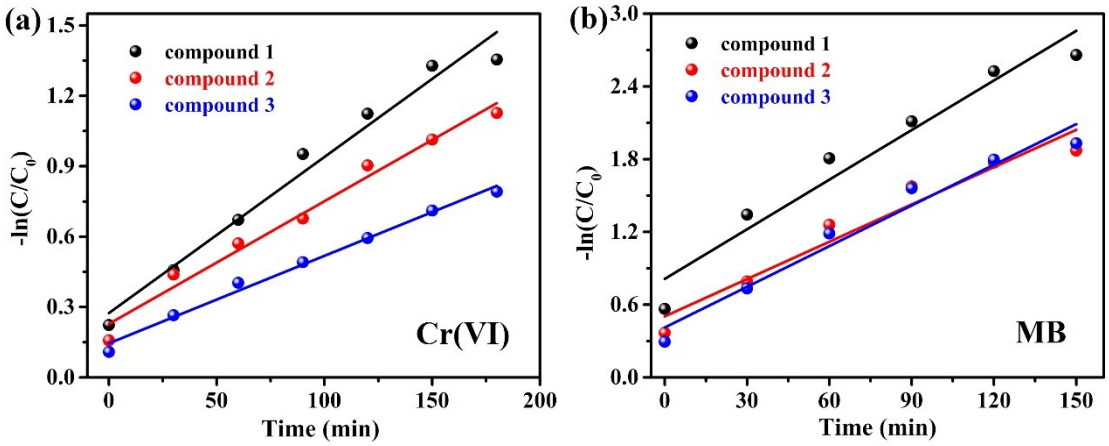


**Fig. S11** The pseudo-first order kinetics plot for the photocatalytic reduction of Cr(VI) (a) and degradation of MB (b).

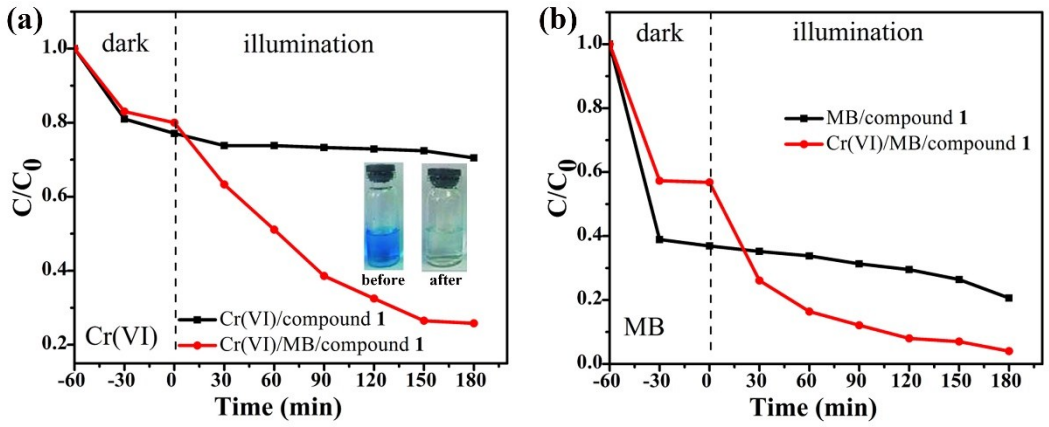


**Fig. S12** Removals of (a) Cr(VI) or (b) MB in single or mixture solution over compound **1** photocatalyst under irradiation.

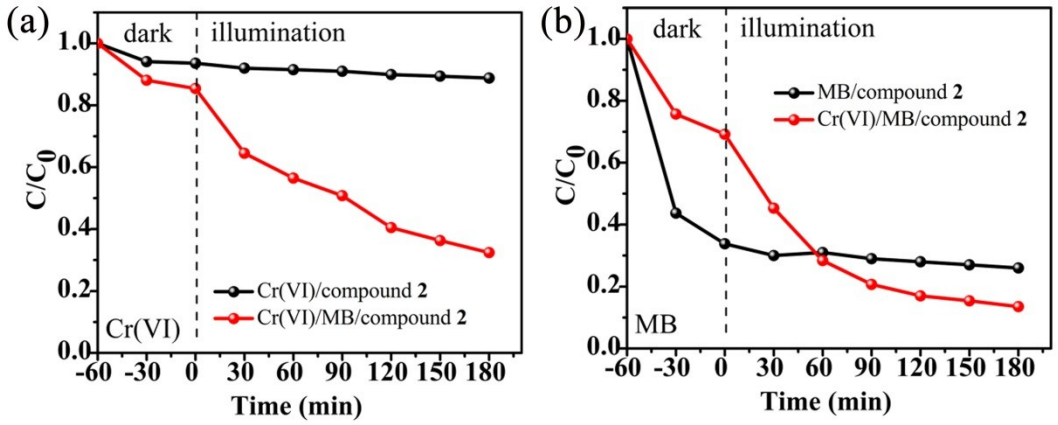


**Fig. S13** Removals of (a) Cr(VI) or (b) MB in single or mixture solution over compound **2** photocatalyst under irradiation.

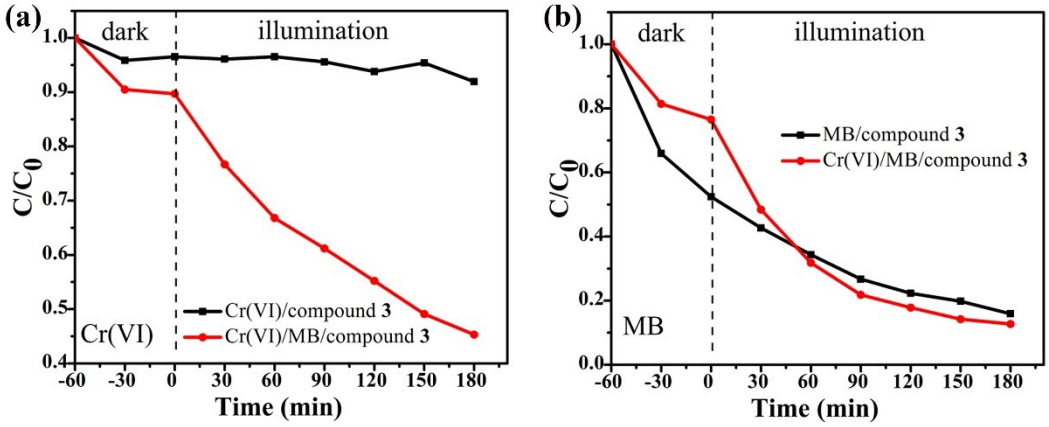


**Fig. S14** Removals of (a) Cr(VI) or (b) MB in single or mixture solution over compound **3** photocatalyst under irradiation.

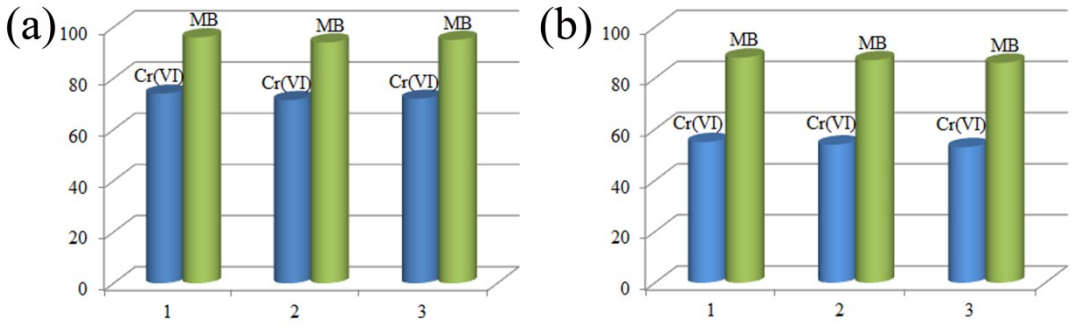


**Fig. S15** Three parallel experiments of compound **1** (a) and **3** (b) photocatalyst under irradiation.

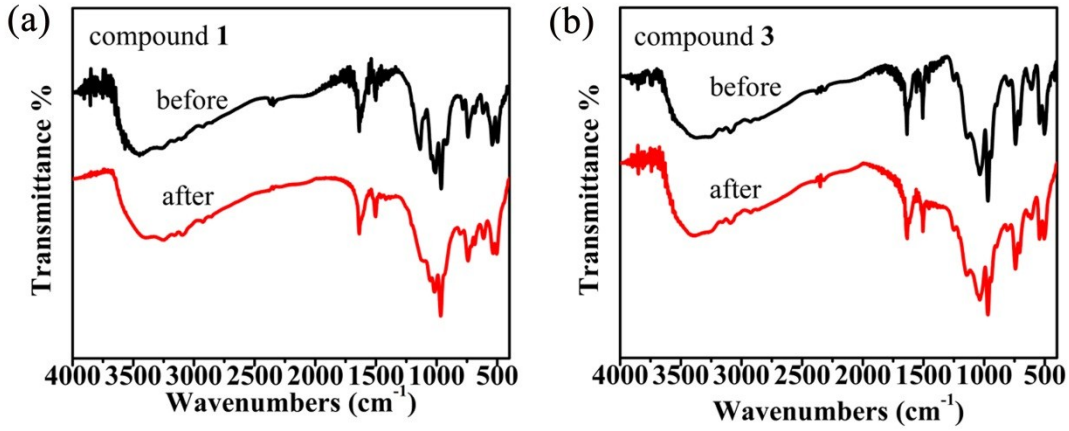


**Fig. S16** Infrared spectra of compounds **1**, **3** before and after catalytic experiments. The slight shift of the absorption peak of 3250-3440 $cm^{-1}$ may stem from the reason that the catalyst is not completely air-dried after catalysis.

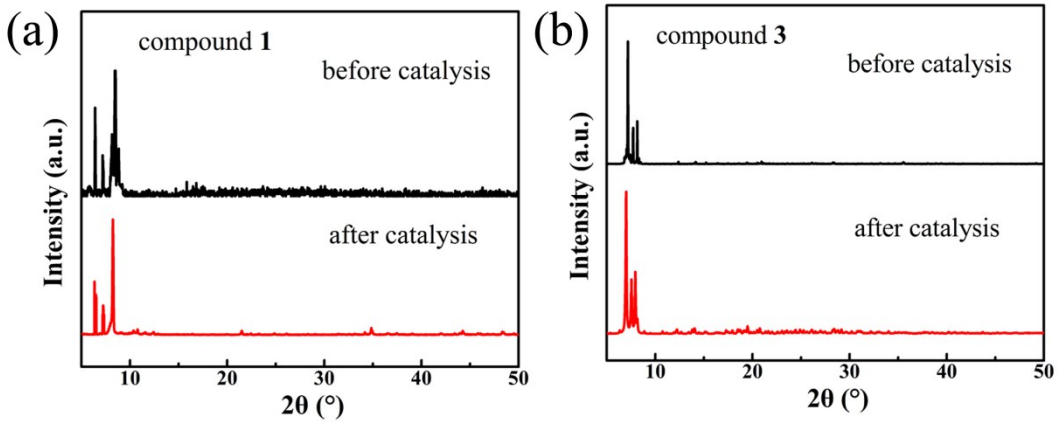


**Fig. S17** The XRD of compounds **1**, **3** before and after catalytic experiments.

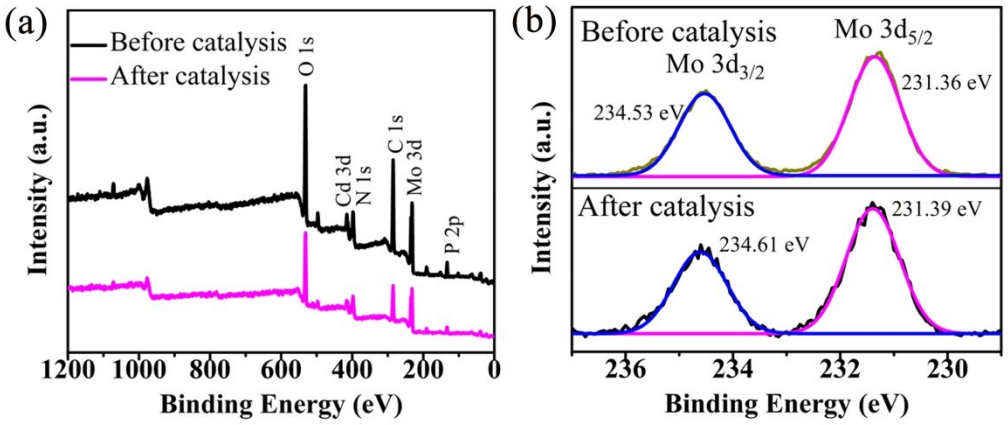


**Fig. S18** XPS spectra of compound **2**: (a) the full survey; (b) Mo 3d XPS of before and after the reaction.

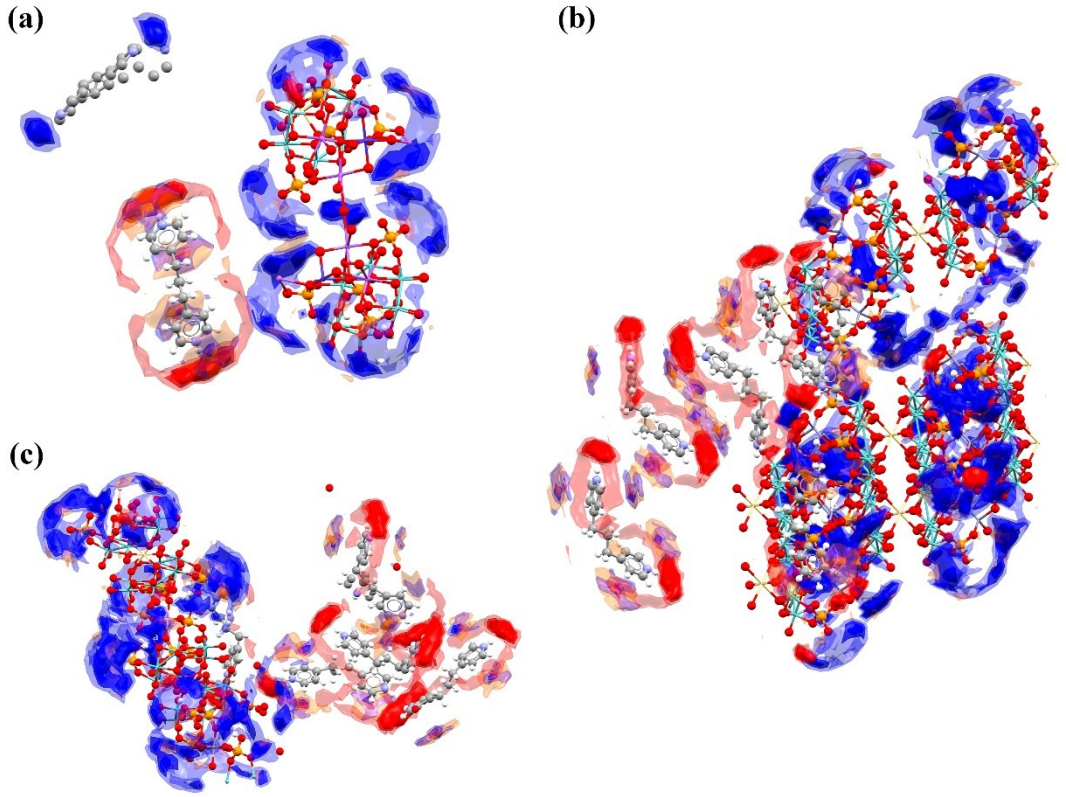


**Fig. S19** The interaction map of compounds **1-3**. The blue area represents the position that can absorb positive charged species and the red area represents the sites that can absorb negative charged species.

## 3. Supplementary Tables

**Table S1.** Crystal data and structure refinement details for compounds **1-3**.

| Compound | **1** | **2** | **3** |
|---|---|---|---|
| Formula | $C_{26}H_{60}Cd_{1.20}Co_{0.80}Mo_{12}N_4Na_4O_{71}P_8$ | $C_{39}H_{72}CdMo_{12}N_6O_{68}P_8Zn_2$ | $C_{65}H_{110}Al_2Cd_2Mo_{24}N_{10}O_{137}P_{16}$ |
| Mr. | 3237.8 | 3355.25 | 6300.47 |
| Cryst. Syst. | Monoclinic | Triclinic | Monoclinic |
| Space group | *C*2/*c* | *P*-1 | *Pn* |
| *a* ( Å ) | 21.0842(6) | 13.126(4) | 15.8820(18) |
| *b* ( Å ) | 18.3743(5) | 25.198(7) | 21.676(2) |
| *c* ( Å ) | 21.9022(6) | 30.034(8) | 25.338(3) |
| $\alpha, \beta, \gamma$ ( ° ) | 90, 100.716(3), 90 | 113.698(4), 101.194(4), 90.634(4) | 90, 94.559(2), 90 |
| Volume ( Å$^3$ ), *Z* | 8337.1(4), 4 | 8879(4), 4 | 8695.4(17), 2 |
| $D_{cale}$ (Mg·m$^{-3}$) | 2.582 | 2.510 | 2.409 |
| $\mu$ (mm$^{-1}$) | 2.492 | 2.658 | 2.182 |
| $F_{(000)}$ | 6241 | 6496 | 6084 |
| Crystal size (mm$^3$) | 0.17 × 0.15 × 0.13 | 0.19 × 0.17 × 0.15 | 0.17 × 0.15 × 0.13 |
| $\theta$ (°) | 3.129 to 25.010 | 2.074 to 25.010 | 1.738 to 25.010 |
| Reflections collected | 15730 | 39555 | 39054 |
| Independent Refl. | 7315 [$R_{(int)}$= 0.0255] | 29329 [$R_{(int)}$= 0.0261] | 19835 [$R_{(int)}$= 0.0256] |
| Max and min. tran. | 0.723 and 0.661 | 0.671 and 0.610 | 0.753 and 0.697 |
| Data/restraints/parameter | 7315 / 643 / 623 | 29329 / 1369 / 2437 | 19835 / 1673 / 2317 |
| GOF on $F^2$ | 1.044 | 1.049 | 1.057 |
| $R_1$, $wR_2$ [$I$ >2σ($I$)] | $R_1$= 0.0423, $wR_2$= 0.1122 | $R_1$=0.0468, $wR_2$= 0.1188 | $R_1$= 0.0334, $wR_2$= 0.0883 |
| $R_1$, $wR_2$ (all data) | $R_1$= 0.0488, $wR_2$= 0.1173 | $R_1$= 0.0661, $wR_2$= 0.1312 | $R_1$= 0.0374, $wR_2$= 0.0925 |

**Table S2.** Selected bond lengths (Å) and bond angles (º) of compound **1**.

| | | | | | |
|---|---|---|---|---|---|
| Mo(1)-O(27) | 1.677(5) | Mo(5)-O(21) | 1.680(5) | P(2)-O(14) | 1.534(5) |
| Mo(1)-O(8) | 1.937(5) | Mo(5)-O(19) | 1.927(5) | P(2)-O(10) | 1.550(5) |
| Mo(2)-O(9) | 1.675(5) | Mo(6)-O(15) | 1.676(5) | P(3)-O(30) | 1.576(5) |
| Mo(2)-O(3) | 1.935(5) | Mo(6)-O(8) | 1.925(5) | P(4)-O(25) | 1.494(6) |
| Mo(3)-O(22) | 1.679(5) | Cd(1)-O(11) | 2.196(5) | Na(1)-O(17) | 2.425(7) |
| Mo(3)-O(19) | 1.939(5) | Cd(1)-O(6) | 2.198(4) | Na(1)-O(1) | 2.460(6) |
| Mo(4)-O(10) | 2.079(5) | P(1)-O(20) | 1.541(5) | Na(2)-O(4W) | 2.727(7) |
| Mo(4)-O(7) | 2.124(5) | P(1)-O(13) | 1.551(5) | O(30)-Na(1)#2 | 2.528(7) |
| O(2)-Mo(1)-O(26) | 158.3(2) | O(15)-Mo(6)-O(8) | 106.4(2) | Na(1)-P(1)-Na(2) | 78.26(5) |
| O(27)-Mo(1)-O(8) | 106.5(2) | O(8)-Mo(6)-O(2) | 95.2(2) | O(17)-P(2)-O(10) | 111.7(3) |
| O(9)-Mo(2)-O(6) | 101.4(2) | O(2)-Cd(1)-O(2)#1 | 180.0 | O(31)-P(3)-O(29) | 113.1(3) |
| O(22)-Mo(3)-O(11) | 100.3(2) | Na(2)-Cd(2)-Na(2)#2 | 180.0 | O(25)-P(4)-O(23) | 112.9(3) |
| O(16)-Mo(4)-O(6) | 102.4(2) | P(2)-Na(1)-Cd(2) | 97.37(8) | P(1)-O(20)-Mo(1) | 127.2(3) |
| O(3)-Mo(4)-O(6) | 95.3(2) | O(26)-Na(2)-O(1) | 106.2(3) | Mo(1)-O(26)-Na(2) | 100.3(2) |
| O(21)-Mo(5)-O(11) | 102.9(2) | O(1)-Na(2)-O(3w) | 96.5(4) | P(3)-O(29)-Mo(2) | 130.1(3) |
| O(19)-Mo(5)-O(11) | 95.8(2) | O(1w)-Na(2)-O(4w) | 97.5(4) | P(3)-O(31)-Cd(2) | 156.1(3) |

Symmetry transformations used to generate equivalent atoms: #1 -x+3/2,-y+3/2,-z+2; #2 -x+2,-y+1,-z+2

**Table S3.** Selected bond lengths (Å) and bond angles (º) of compound **2**.

| | | | | | |
|---|---|---|---|---|---|
| Mo(1)-O(1) | 1.687(6) | Mo(8)-O(42) | 1.677(6) | Mo(24)-O(103) | 2.292(5) |
| Mo(1)-O(3) | 1.951(5) | Mo(8)-O(43) | 1.945(5) | P(1)-O(23) | 1.544(5) |
| Mo(2)-O(3) | 1.958(5) | Mo(10)-O(57) | 1.688(6) | P(4)-O(32) | 1.582(6) |
| Mo(2)-O(2) | 1.969(5) | Mo(10)-O(60) | 1.954(5) | P(5)-O(37) | 1.542(5) |
| Mo(3)-O(17) | 1.688(6) | Mo(11)-O(49) | 1.695(5) | P(6)-O(30) | 1.591(6) |
| Mo(3)-O(21) | 1.937(5) | Mo(11)-O(45) | 1.954(5) | P(7)-O(38) | 1.524(5) |
| Mo(4)-O(21) | 1.936(5) | Mo(13)-O(63) | 1.703(5) | P(10)-O(85) | 1.574(6) |
| Mo(4)-O(15) | 1.978(5) | Mo(14)-O(76) | 2.285(5) | P(11)-O(68) | 1.512(6) |
| Mo(5)-O(27) | 1.707(5) | Mo(15)-O(90) | 1.682(6) | P(12)-O(82) | 1.571(6) |
| Mo(5)-O(26) | 1.938(5) | Mo(16)-O(77) | 2.315(5) | P(13)-O(110) | 1.535(5) |
| Mo(6)-O(26) | 1.959(5) | Mo(19)-O(94) | 1.701(5) | P(16)-O(121) | 1.568(6) |
| Mo(6)-O(12) | 1.986(5) | Mo(20)-O(105) | 2.337(5) | Cd(1)-O(15) | 2.279(5) |
| Mo(7)-O(50) | 1.704(6) | Mo(21)-O(117) | 1.697(5) | Cd(2)-O(55) | 2.270(5) |
| Mo(7)-O(43) | 1.932(5) | Mo(22)-O(109) | 2.320(5) | Cd(3)-O(72) | 2.313(5) |
| Zn(1)-O(18) | 1.943(5) | Zn(3)-O(79) | 1.949(5) | Zn(4)-O(110) | 1.946(5) |
| Zn(2)-O(37) | 161.7(4) | Zn(3)-O(97) | 1.951(6) | Zn(4)-O(87)#1 | 1.957(5) |
| O(1)-Mo(1)-O(3) | 106.9(3) | O(44)-Mo(12)-Mo(1) | 88.68(1) | O(51)-P(5)-O(52) | 107.6(3) |
| O(6)-Mo(2)-O(2) | 102.5(3) | O(90)-Mo(15)-O(84) | 105.7(3) | O(59)-P(8)-O(61) | 111.4(3) |
| O(17)-Mo(3)-O(21) | 106.2(3) | O(77)-Mo(16)-Mo(5) | 88.13(1) | O(71)-P(9)-O(7) | 107.6(3) |
| O(11)-Mo(6)-O(12) | 101.4(2) | O(106)-Mo(23)-O(1) | 180.0 | O(120)-P(16)-O(122) | 109.4(3) |
| O(50)-Mo(7)-O(43) | 108.3(3) | O(13)-Mo(24)-Mo(3) | 180.0(3) | O(15)-Cd(1)-O(15)#2 | 180.0 |
| O(44)-Mo(8)-Mo(7) | 88.75(12) | O(23)-P(1)-O(16) | 106.7(8) | O(55)#3-Cd(2)-O(55) | 180.0 |
| O(58)-Mo(9)-O(60) | 106.5(3) | O(7)-P(2)-O(13) | 109.0(3) | O(73)#4-Cd(3)-O(73) | 180.0(3) |
| O(38)-Zn(2)-O(37) | 116.4(2) | O(68)-Zn(3)-O(97) | 102.0(3) | O(83)-Zn(4)-O(111) | 96.5(2) |

Symmetry transformations used to generate equivalent atoms: #1 x-1,y,z; #2 -x+2,-y+1,-z+1; #3 -x+1,-y,-z+1; #4 -x+1,-y+1,-z+2

**Table S4.** Selected bond lengths (Å) and bond angles (º) of compound **3**.

| | | | | | |
|---|---|---|---|---|---|
| Mo(1)-O(54) | 1.669(9) | Mo(15)-O(108) | 2.085(8) | P(4)-O(102) | 1.517(9) |
| Mo(2)-O(19) | 1.945(9) | Mo(18)-O(80) | 1.682(10) | P(6)-O(109) | 1.495(9) |
| Mo(3)-O(72) | 1.670(9) | Mo(19)-O(37) | 2.229(9) | P(7)-O(37) | 1.563(9) |
| Mo(4)-O(101) | 1.938(9) | Mo(22)-O(28) | 1.970(9) | P(9)-O(121) | 1.529(10) |
| Mo(5)-O(48) | 1.691(10) | Mo(23)-O(35) | 2.278(9) | P(10)-O(43) | 1.498(9) |
| Mo(6)-O(95) | 1.925(9) | Cd(1)-O(9) | 2.256(9) | P(11)-O(90) | 1.547(12) |
| Mo(7)-O(36) | 1.672(10) | Cd(2)-O(28) | 2.254(8) | P(12)-O(52) | 1.483(11) |
| Mo(8)-O(95) | 1.918(8) | Al(2)-O(40) | 1.862(9) | P(13)-O(71) | 1.536(11) |
| Mo(9)-Mo(19) | 2.6190(17) | P(1)-O(26) | 1.701(5) | P(14)-O(119) | 1.468(13) |
| Mo(10)-O(65) | 1.671(10) | P(1)-O(96) | 2.337(5) | P(14)-O(123) | 1.486(15) |
| Mo(11)-Mo(18) | 2.5901(14) | P(2)-O(56) | 1.475(10) | P(15)-O(55) | 1.474(9) |
| Mo(12)-O(116) | 1.683(10) | P(2)-O(59) | 1.523(10) | P(15)-O(67) | 1.516(10) |
| Mo(13)-Mo(14) | 2.5973(17) | P(3)-O(60) | 1.495(11) | P(16)-O(40) | 1.509(8) |
| Mo(14)-O(122) | 1.665(10) | P(3)-O(92) | 1.506(11) | P(16)-O(21) | 1.515(8) |
| O(54)-Mo(1)-O(101) | 105.1(5) | O(5)-Mo(14)-Mo(13) | 86.4(2) | O(6)-P(1)-O(96) | 113.9(5) |
| O(53)-Mo(2)-O(20) | 102.2(5) | O(76)-Mo(17)-O(29) | 170.0(4) | O(6)-P(2)-O(58) | 114.8(6) |
| O(72)-Mo(3)-O(104) | 106.2(5) | O(1)-Mo(18)-Mo(11) | 88.5(2) | O(6)-P(3)-O(92) | 109.3(7) |
| O(44)-Mo(4)-O(3) | 102.1(5) | O(9)-Mo(21)-O(17) | 107.0(5) | O(2)-P(4)-O(25) | 107.9(5) |
| O(48)-Mo(5)-O(111) | 104.4(5) | O(5)-Mo(22)-Mo(20) | 87.7(2) | O(1)-P(5)-O(73) | 104.9(5) |
| O(114)-Mo(6)-O(9) | 101.6(4) | O(10)-Cd(1)-O(9) | 179.8(4) | O(3)-P(8)-O(14) | 110.1(7) |
| O(37)-Mo(7)-Mo(21) | 88.4(2) | O(7)-Cd(1)-O(3) | 179.7(4) | O(6)-P(9)-O(70) | 111.0(6) |
| O(118)-Mo(8)-O(95) | 106.5(5) | O(28)-Cd(2)-O(27) | 178.9(4) | O(9)-P(10)-O(9) | 104.2(6) |
| O(33)-Mo(12)-O(8) | 95.4(4) | O(34)-Al(2)-O(55) | 94.1(5) | O(6)-P(15)-O(9) | 106.9(5) |
| O(63)-Mo(13)-O(5) | 94.4(5) | O(34)-Al(2)-O(40) | 97.3(4) | O(4)-P(1)-O(21) | 112.7(5) |

**Table S5.** BVS calculations of Mo, P and M centers in compounds **1-3**.

| | | | | | | | | | | | | |
|---|---|---|---|---|---|---|---|---|---|---|---|---|
| **1** | Mo1 | Mo2 | Mo3 | Mo4 | Mo5 | Mo6 | P1 | P2 | P3 | P4 | Cd1 | Cd2 |
| | 5.220 | 5.257 | 5.220 | 5.252 | 5.286 | 5.268 | 4.866 | 4.845 | 4.856 | 4.815 | 2.661 | 2.314 |
| **2** | Mo1 | Mo2 | Mo3 | Mo4 | Mo5 | Mo6 | Mo7 | Mo8 | Mo9 | Mo10 | Mo11 | Mo12 |
| | 5.025 | 5.052 | 5.036 | 5.019 | 4.926 | 5.071 | 4.981 | 5.064 | 4.975 | 5.068 | 4.997 | 5.024 |
| | Mo13 | Mo14 | Mo15 | Mo16 | Mo17 | Mo18 | Mo19 | Mo20 | Mo21 | Mo22 | Mo23 | Mo24 |
| | 5.002 | 4.958 | 5.092 | 5.044 | 5.035 | 5.116 | 4.980 | 5.119 | 4.995 | 5.052 | 5.070 | 5.037 |
| | P1 | P2 | P3 | P4 | P5 | P6 | P7 | P8 | P9 | P10 | P11 | P12 |
| | 4.623 | 4.736 | 4.651 | 4.790 | 4.601 | 4.757 | 4.694 | 4.745 | 4.618 | 4.717 | 4.692 | 4.814 |
| | P13 | P14 | P15 | P16 | Cd1 | Cd2 | Cd3 | Cd4 | Zn1 | Zn2 | Zn3 | Zn4 |
| | 4.581 | 4.777 | 4.717 | 4.736 | 2.141 | 2.123 | 2.131 | 2.146 | 2.052 | 2.012 | 2.094 | 2.022 |
| **3** | Mo1 | Mo2 | Mo3 | Mo4 | Mo5 | Mo6 | Mo7 | Mo8 | Mo9 | Mo10 | Mo11 | Mo12 |
| | 5.344 | 5.308 | 5.344 | 5.295 | 5.221 | 5.407 | 5.271 | 5.429 | 5.351 | 5.294 | 5.282 | 5.351 |
| | P1 | P2 | P3 | P4 | P5 | P6 | P7 | P8 | P9 | P10 | P11 | P12 |
| | 4.918 | 4.915 | 5.048 | 4.908 | 4.985 | 4.905 | 4.849 | 4.885 | 4.888 | 4.981 | 4.885 | 5.213 |
| | P13 | P14 | P15 | P16 | Cd1 | Cd2 | Al1 | Al2 | | | | |
| | 4.817 | 5.334 | 5.044 | 5.959 | 2.300 | 2.237 | 3.189 | 3.204 | | | | |

**Table S6.** Selected hydrogen bonding lengths and angles for compound **1**.

| Donor-H···Acceptor | D-H [Å] | H...A [Å] | D...A [Å] | D-H...A [°] |
|---|---|---|---|---|
| N(1)-H(1)···O(7$^{i}$) | 0.86 | 1.98 | 2.780(11) | 154 |
| O(5)-H(5D)···O(6$^{ii}$) | 0.94 | 1.89 | 2.810(7) | 163 |
| O(7)-H(7D)···O(2$^{ii}$) | 0.83 | 1.92 | 2.742(8) | 169 |
| O(12)-H(12D)···O(2) | 0.75 | 2.56 | 2.800(6) | 101 |
| O(12)-H(12D)···O(6) | 0.75 | 2.52 | 2.803(7) | 105 |
| O(12)-H(12D)···O(11$^{ii}$) | 0.75 | 2.08 | 2.829(6) | 177 |
| O(18)-H(18)···N(2$^{iii}$) | 0.82 | 2.57 | 3.164(19) | 131 |
| O(18)-H(18)···N(2$^{iv}$) | 0.82 | 2.22 | 2.99(2) | 156 |
| O(24)-H(24)···N(3w) | 0.82 | 2.45 | 3.224(17) | 157 |
| C(3)-H(3)···O(22$^{v}$) | 0.93 | 2.29 | 3.162(12) | 156 |

Symmetry codes: i = 1-x,y,3/2-z; ii = 3/2-x,3/2-y,2-z; iii = 1-x,1-y,2-z; iv = 1/2+x,-1/2+y,z; v = 1-x,1-y,1-z.

**Table S7.** Selected hydrogen bonding lengths and angles for compound **2**.

| Donor-H···Acceptor | D-H [Å] | H...A [Å] | D...A [Å] | D-H...A [°] |
|---|---|---|---|---|
| N(1)-H(1A)···O(54$^{i}$) | 0.86 | 2.30 | 2.938(14) | 131 |
| N(2)-H(2A)···O(65$^{ii}$) | 0.86 | 2.02 | 2.840(10) | 159 |
| N(3)-H(3)···O(5$^{iii}$) | 0.86 | 2.01 | 2.791(10) | 150 |
| N(4)-H(4A)···O(93$^{iv}$) | 0.86 | 2.12 | 2.875(15) | 146 |
| N(5)-H(5A)···O(114$^{v}$) | 0.86 | 2.05 | 2.806(12) | 145 |
| N(7)-H(7)···O(41) | 0.86 | 2.04 | 2.831(11) | 153 |
| N(9)-H(9A)···O(75$^{vi}$) | 0.86 | 2.10 | 2.940(12) | 167 |
| N(11)-H(11)···O(37) | 0.86 | 2.16 | 2.991(12) | 162 |
| O(13)-H(13)···O(53$^{vii}$) | 0.82 | 2.10 | 2.834(8) | 149 |
| O(32)-H(32)···O(23) | 0.82 | 2.28 | 2.989(9) | 145 |
| C(4)-H(4)···O(56$^{iv}$) | 0.93 | 2.49 | 3.272(12) | 141 |
| C(12)-H(12)···O(57$^{iv}$) | 0.93 | 2.41 | 3.234(11) | 147 |
| C(17)-H(17)···O(101$^{viii}$) | 0.93 | 2.32 | 3.137(11) | 146 |
| C(22)-H(22)···O(94$^{v}$) | 0.93 | 2.49 | 3.410(16) | 169 |
| C(53)-H(53)···O(74 $^{vi}$) | 0.93 | 2.37 | 3.178(15) | 146 |

Symmetry codes: i = -1+x,1+y,z; ii = 1-x,1-y,1-z; iii = 2-x,1-y,1-z; iv = x,1+y,z; v = -x,1-y,2-z; vi = -1+x,y,z; vii = 1+x,y,z; viii = 1+x,1+y,z.

**Table S8.** Selected hydrogen bonding lengths and angles for compound **3**.

| Donor-H···Acceptor | D-H [Å] | H...A [Å] | D...A [Å] | D-H...A [°] |
|---|---|---|---|---|
| N(1)-H(1A)···O(60$^{i}$) | 0.86 | 2.08 | 2.86(2) | 151 |
| N(5)-H(5A)···O(5$^{ii}$) | 0.86 | 1.92 | 2.748(17) | 161 |
| N(6)-H(6)···O(1$^{iii}$) | 0.86 | 1.95 | 2.766(19) | 158 |
| N(9)-H(9A)···O(33$^{iv}$) | 0.86 | 1.88 | 2.730(15) | 169 |
| O(47)-H(47)···O(84) | 0.82 | 1.88 | 2.618(13) | 149 |
| O(75)-H(75)···O(30) | 0.82 | 2.37 | 2.972(14) | 130 |
| O(99)-H(99)···O(19) | 0.82 | 1.89 | 2.634(13) | 151 |
| C(22)-H(22)···O(4$^{v}$) | 0.93 | 2.46 | 3.31(3) | 152 |
| C(27)-H(27)···O(72 $^{ii}$) | 0.93 | 2.33 | 3.20(2) | 156 |
| C(39)-H(39)···O(77$^{iii}$) | 0.93 | 2.32 | 3.14(2) | 146 |
| C(53)-H(53)···O(92$^{iv}$) | 0.93 | 2.03 | 2.93(2) | 161 |

Symmetry codes: i = x,-1+y,z; ii = -1/2+x,1-y,-1/2+z; iii = x,y,-1+z; iv = x,-1+y,-1+z; v = 1/2+x,1-y,-1/2+z.

**Table S9.** Peak potential data (mV) for each peak of compounds **1-3** at a sweep speed of 140 mV·s$^{-1}$.

| Scan rate<br>140 mV s$^{-1}$ | *Ea*/*Ec* (I) / mV<br>$E_{1/2}$, $\Delta E$ | *Ea*/*Ec* (II) / mV<br>$E_{1/2}$, $\Delta E$ | *Ea*/*Ec* (III) / mV<br>$E_{1/2}$, $\Delta E$ | *Ea*/*Ec* (IV) / mV |
|---|---|---|---|---|
| Compound **1** | 15 / -35<br>-10, 50 | 261/ 223<br>242, 38 | 415 / 368<br>392, 47 | -133 |
| Compound **2** | 8 / -28<br>-10, 36 | 260 / 229<br>245, 31 | 420 / 369<br>395, 51 | -129 |
| Compound **3** | 16 / -30<br>-7, 46 | 262 / 227<br>245, 35 | 427 / 373<br>400, 54 | -130 |

**Table S10.** Comparison of pollutant removal with various other reported POM-based materials.

| catalyst | time (min) | pollutants | light source | conversion (%) | ref |
|---|---|---|---|---|---|
| **Crystal 1** | **180** | **Cr(VI)-MB** | **visible** | **74%-96%** | **This work** |
| $[Cu_4(\mu_3\text{-}OH)_2(H_2O)_6(4\text{-}dpye)_2(TeMo_6O_{24})]\cdot 2H_2O$ | 90 | MB | UV | 73% | 1 |
| $[Cd3(2,3'\text{-}Htmbpt)_2(2,3'\text{-}tmbpt)_4(\gamma\text{-}Mo_8O_{26})(\beta\text{-}Mo_8O_{26})(H_2O)_4]\cdot 5H_2O$ | 120 | MB | UV | 56% | 2 |
| $[Ag(phen)_2]_2(Agphen)_2SiW_{12}O_{40}$ | 210 | MB | UV | 70% | 3 |
| $PPy@Ag_{29}SiW_{12}$ | 360 | RhB | UV | 48% | 4 |
| $WO_{3\text{-}X}/NC$ | 90 | VOC | visible | 92% | 5 |
| $[Ag_4(H_2O)(L)_3(SiW_{12}O_{40})]$ | 160 | Cr(VI) | visible | 99% | 6 |
| $Ag/Ag_xH_{3-x}PMo_{12}O_{40}$ | 40 | Cr(VI) | visible | 68% | 7 |
| $PMo_{12}/TiO_2/Ag\text{-}X$ | 60 | Cr(VI) | visible | 71% | 8 |
| $SiW_{12}O_{40}H_4$ | 600 | Cr(VI)-RhB | visible | 75%-99% | 9 |

**Table S11.** The summary of Zeta potential of the reported POM-based complexes.

| POM-based complexes | Zeta potential/ ζ mV | pH | ref |
|---|---|---|---|
| $[\alpha\text{-}PW_{11}O_{39}Fe^{III}]^{4-}$-O－-ligated hematite-core complex | -40±5 | 8 | 10 |
| $\{[Cu(H_2biim)_2][\{Cu(H_2biim)_2(H_2O)\}_2Cu_2biim)(H_2O)_2]\text{-}H[(\{Cu(H_2biim)(H_2O)_2\}_{0.5})_2((C_3HN_2Cl_2)\{Cu(H_2biim)\}_2)\{Na(H_2O)P_5W_{30}O_{110}\}]\cdot xH_2O\}n$ | -30 | 3.5-8.5 | 11 |

| | | | |
|---|---|---|---|
| P2W18/MIL-101(Cr) | -12.5 | - | 12 |
| $[PBI]_5Ru_4POM$ | -39.9 | 8 | 13 |
| CitNPs@POV | -49.6±1.7 | | 14 |
| $C_{16}IPS/Mo_7$ | -40 | - | 15 |

References:


[1] X. L. Wang, J. J. Sun, H. Y. Lin, Z. H. Chang, X. Bai and X. Wang, Polyhedron, 2017, **124**, 30-40.

[2] W. Q. Kan, S. Z. Wen, Y. H. Kan, H. Y. Hu, S. Y. Niu and X. Y. Zhang, Synthetic Met., 2014, **198**, 51-58.

[3] H. J. Pang, Y. Niu, J. Yu, H. Y. Ma, Q. F. Song and S. B. Li, Inorg. Chem. Commun., 2015, **59**, 5-8.

[4] J. Q. Sha, X. Y. Yang, N. Sheng, G. D. Liu, J. S. Li and J. B. Yang, J. Solid State Chem., 2018, **263**, 52-59.

[5] L. Y. Wang, X. X. Xu, S. J. Wu and F. Cao, Catal. Sci. Technol., 2018, **8**, 1366-1374.

[6] H. Zhang, J. Yang, Y. Y. Liu, S. Y. Song, X. L. Liu and J. F. Ma, Dyes Pigments, 2016, **133**, 189-200.

[7] H. F. Shi, G. Yan, Y. Zhang, H. Q. Tan, W. Z. Zhou, Y. Y. Ma, Y. G. Li, W. L. Chen and E. B. Wang, ACS Appl. Mater. Inter., 2017, **9**, 422-430.

[8] S. Kim, J. Yeo and W. Choi, Appl. Catal. B: Environ., 2008, **84**, 148-155.

[9] H. F. Shi, Y. C. Yu, Y. Zhang, X. J. Feng, X. Y. Zhao, H. Q. Tan, S. U. Khan, Y. G. Li and E. B. Wang, Appl. Catal. B, 2018, 221, 280-289

[10] B. Chakraborty, G. Gan-Or, Y. Duan, M. Raula, I. A. Weinstock, Angew. Chem. Int. Ed., 2019, 58, 6584-6589.

[11] J. Du, M. D. Cao, S. L. Feng, F. Su, X. J. Sang, L. C. Zhang, W. S. You, M. Yang, Z. M. Zhu, Chem. Eur. J. 2017, 23, 14614 – 14622.

[12] A. Jarrah, S. Farhadi, Acta Chim. Slov., 2019, 66, 85–102.

[13] M. Bochino, Z. Syrgiannis, M. Burian, N. Marino, E. Pizzolato, K. Dirian, F. Rigodanza, G. A. Volpato, G. Ganga, N. Demitri, S. Berardi, H. Amenitsch, D. M. Guldi, S. Caramori, C. A. Bignozzi, A. Sartorel, M. Prato, Nat. Chem., 2019, 11, 146–153.

[14] S. Tomane, E. Lopez-Maya, S. Boujday, V. Humblot, J. Marrot, N. Rabasso, J. Castells-Gil, C. Sicard, A. Dolbecq, P. Mialane, A. Vallee, Nanoscale Adv., 2019, 1, 3400-3405.

[15] N. Sun, A. L. Wu, Y. Yu, X. P. Gao, L. Q. Zheng, Chem. Eur. J. 2019, 25, 6203-6211.